APPLICATION NOTE

Multi-parametric assessment of EGF treatment effects on signaling pathways, growth and proliferation using AlphaLISA *SureFire Ultra* and cellular imaging.

Author

Jeanine Hinterneder, Ph.D.

Revvity, Inc.

Introduction

When developing models for studying treatment effects on intracellular signaling pathways, it is extremely important to know how your compound will affect various cellular processes. A lot of time, reagents, and cellular material can be saved by concurrently assessing signaling pathways along with cell health and proliferation using high content imaging techniques. Traditional methods of cell signaling analysis, such as Western blot and ELISAs, can be cumbersome and time-consuming, requiring large samples, more effort and longer preparation time. To demonstrate a more efficient cell-based workflow, we used homogeneous, no-wash methods to probe multiple signaling pathways together with cellular imaging and ATP measurement to assess cell growth and viability using a widely accepted Epidermal Growth Factor Receptor (EGFR) model.

EGFR is a long-studied receptor tyrosine kinase commonly upregulated or inappropriately activated in many cancers and is a prominent target for development of therapeutics. EGFR signaling produces complex, varied effects depending on the stimulating ligand and co-receptors expressed and noncanonical functions are currently still being elucidated.[1] Epidermal Growth Factor (EGF) can stimulate changes in cell proliferation, differentiation, growth, migration and apoptosis pathways through the downstream activation of numerous signaling pathways and phosphorylation of thousands of proteins.[2] In this application note, effects of EGF treatment were assessed in a cellular model of human skin cancer. Treatment effects on several intracellular signaling pathways, illustrated in Figure 1A, were examined over a 24-hour period using AlphaLISA™ *SureFire*® *Ultra* assays.

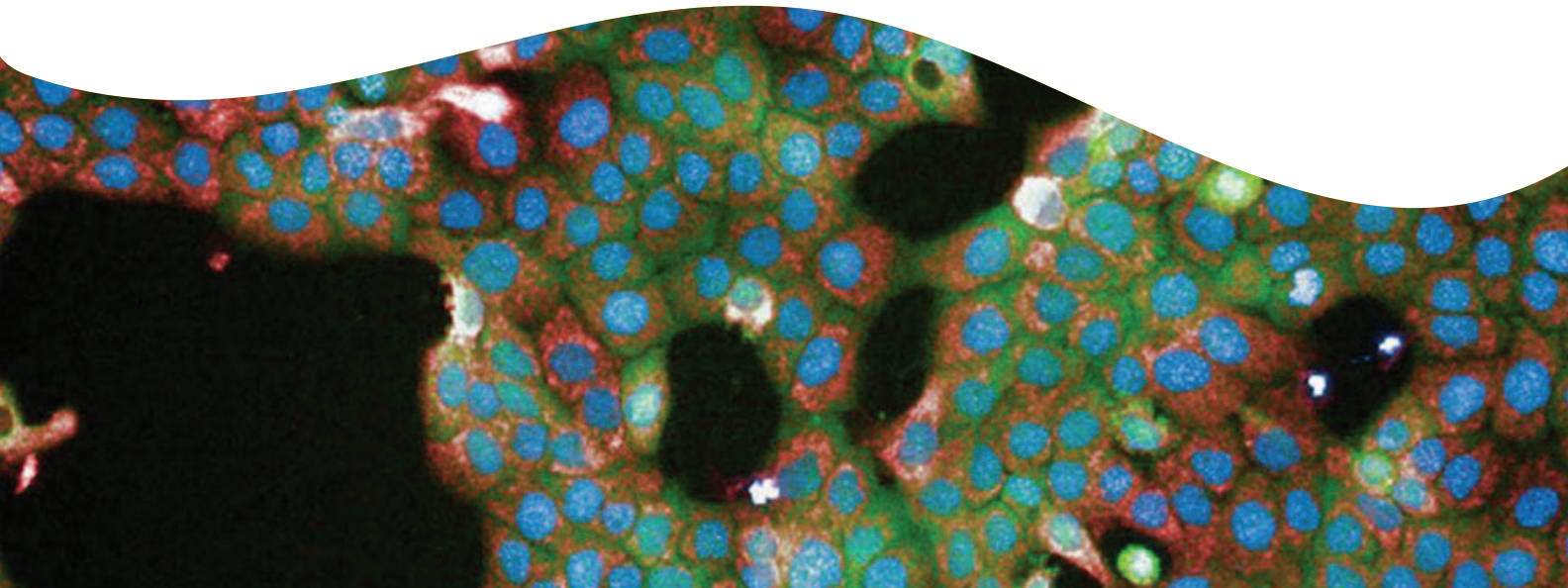

To determine concurrent time-dependent effects of different EGF concentrations on cellular health and proliferation, ATP concentrations were assessed with ATPlite™ 1step luminescence assay and cultures were fluorescently labeled, imaged and analyzed using the Operetta CLS™ high-content analysis system.

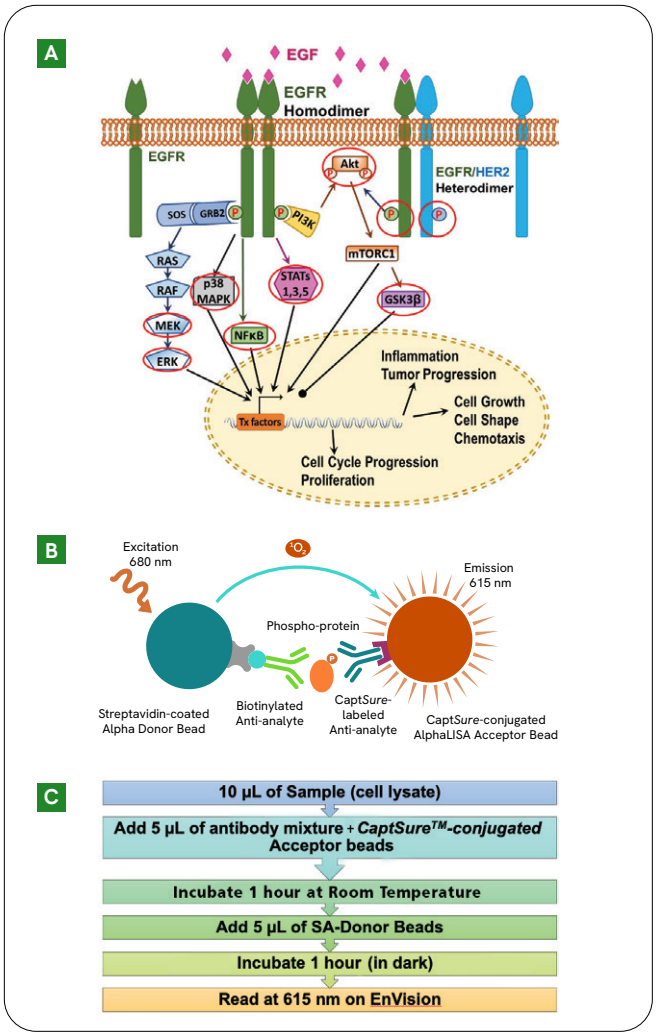

Figure 1. **EGFR signaling pathways and AlphaLISA *SureFire Ultra* assays.** A) Representative model of EGFR signaling highlighting the major signaling pathways studied and specific phosphoproteins (in red circles) assessed in this study. B) Schematic representation of an AlphaLISA *SureFire Ultra* assay for the detection of phosphorylated protein. C) *SureFire Ultra* assay workflow with total incubation time of two hours.

AlphaLISA *SureFire Ultra* technology allows for the detection of molecules of interest in a rapid, homogeneous (mix-andread), no-wash format. In the assay illustrated and outlined in Figure 1B-C, a biotinylated anti-target antibody binds to streptavidin-coated Alpha Donor beads while another antiphosphorylation- site specific antibody, tagged with proprietary CaptSure™ technology, binds to CaptSure-conjugated AlphaLISA Acceptor beads.

Binding the target analyte brings the Donor and Acceptor beads into proximity so that excitation of the Donor beads with light at 680 nm provokes singlet oxygen release which activate nearby Acceptor beads to emit light at 615 nm. This light emission is proportional to the relative amount of total or phosphorylated protein in each sample.

Materials and methods

Cell culture and treatment

The human epidermoid carcinoma-derived cell line A431 (A-431; ATCC® CRL-1555™) was cultured in D-MEM (ATCC #30-2002) supplemented with 10% FBS (ThermoFisher #11875-093). Cells were seeded into white, 384-well ViewPlates™ (Revvity #6007480) at 10,000 cells per well in 25 µL (or 20,000 cells for phospho-AKT experiments) and allowed to attach overnight. Treatment was administered the next day as varying concentrations of EGF (rh EGF; R&D Systems #236-EG-200) diluted in culture media and cells were assessed at different timepoints.

AlphaLISA *SureFire Ultra* assays

After exposure to EGF for varying amounts of time (five minutes to one day) media were removed (aspirated) and cells lysed by the addition of 10 µL/well *Surefire Ultra* Lysis Buffer. Plates were shaken at room temperature for 10 minutes on a DELFIA™ PlateShaker set at 600-700 RPM, sealed, and frozen at -20°C. Samples were thawed and AlphaLISA *SureFire Ultra* Assays were performed at room temperature as described in the kit manual (as shown in Figure 1C). A white adhesive bottom seal (Revvity #6005199, provided with ViewPlates) was applied to reduce well-to-well crosstalk. Multiple assays for different targets were run in parallel wells or separate plates. Data presented here were generated using Revvity's AlphaLISA *SureFire Ultra* assays for the following targets: phospho-EGFR (Tyr1068) (#ALSU-PEGFR-B); p-ErbB2 (Tyr1221/1222) (#ALSUPEB2- A); p-MEK1 (Ser218/222) (#ALSU-PMEK1-A); p-ERK1/2 (Thr202/Tyr204) (#ALSU-PERK-A); phospho-p38 MAPK (Thr180/ Tyr182) (#ALSU-PP38-B); p-AKT1/2/3 (Thr308) (#ALSU-PAKT-B); p-AKT1/2/3 (Ser473) (ALSU-PAKT-A); Total AKT1/2/3 (#ALSUTAKT- B); p-GSK-3β (Ser9) (ALSU-PGS3B-A); p-STAT1 (Tyr701) (ALSU-PST1-A); p-STAT3 (Tyr705) (ALSU-PST3-A); p-STAT5 (Tyr694/699) (ALSU-PST5-B); p-NF-κB (Ser536) (#ALSU-PNKFB-A). Assays were read on the EnVision™ Multimode Plate reader using default settings for Alpha detection.

ATPlite 1Step

For assessing the effect of EGF on ATP concentrations in our cultures, the ATPlite™ 1Step Luminescence Assay (Revvity #6016731) was used as described in the manual. For these experiments, media were removed and cells were rinsed with PBS before addition of reagents. Signals were measured on the EnVision system using settings for ultrasensitive luminescence detection.

Cell staining and imaging

For cellular imaging studies, cells were either labeled by the addition of cell permeable dyes diluted in culture media or fixed for 15 minutes with 4% paraformaldehyde, rinsed and stored in 1X PBS at 4°C for later staining. For labeling live cells, dyes used at indicated final concentrations were: 5 µg/mL Hoechst 33342 (ThermoFisher #H3570) and 0.5 µM MitoTracker™ Deep Red (ThermoFisher #M22426). To assess apoptosis, cells were incubated for 30 minutes in CellEvent™ Caspase-3/7 Green Detection Reagent (ThermoFisher #C10423) at 5 µM in culture media, then fixed and stained with 1 µg/mL DAPI (ThermoFisher #62248) to identify nuclei of all cells. For assessment of Ki-67+ nuclei, fixed cells were permeabilized for 30 minutes with 0.03% Triton-X-100 in 5% Goat Serum and stained for two hours with Ki-67 Rabbit mAb conjugated to AlexaFluor 488 (Cell Signaling Technology #11882) and then counter-stained with DAPI. The Operetta CLS system and Harmony® software were used to image well regions and analyze cellular morphology using either the 10X or 20X LWD objectives and appropriate filters for each fluorescent dye.

Data analysis

Graphs were made using GraphPad® Prism 7. Each datapoint is an average of three wells with error bars indicating standard deviation (unless indicated otherwise).

Results

EGF stimulates receptor phosphorylation

EGF concentrations are tightly regulated and spatially segregated in the human body with common concentrations ranging from 0.1 – 100 ng/mL, so it is important to assess the effects of a wide range of EGF concentrations when developing cell culture models.[2,3] Ligand-activation of the EGFR leads to the autophosphorylation of multiple tyrosine residues on the intracellular C-terminal tail, including Tyrosine 1068, whose phosphorylation is a biomarker predictive of drug sensitivity in a lung cancer model.[4] To determine the effects of EGF on EGFR phosphorylation, A431 cells were treated with a broad range of EGF concentrations for 10 minutes, one hour, and one day and assayed for effects on EGFR phosphorylation (at Tyr1068) using AlphaLISA *SureFire Ultra.* The resulting data, shown in Figure 2A, illustrate the rapid phosphorylation of the EGFR and dose-dependent increases in activation at concentrations of 0.5 ng/mL and above. Also illustrated is the large signal-to-background (S/B) offered by these assays. In order to compare the data from different treatment timepoints or for different phosphoproteins, raw AlphaLISA data were normalized to control wells receiving no EGF (media only) and shown as "% of No EGF Control" (Figure 2B).

The EGFR (ErbB1) is the prototypical member of the ErbB/HER family of receptors (ErbB1-B4) and can heterodimerize with HER2 (ErbB2) leading to transphosphorylation, impacting downstream signaling. Though the HER2 receptor does not have a ligand binding domain, studies have demonstrated that HER2 is expressed in A431 cells and that EGF induces HER2 receptor phosphorylation.[5] We observe here (Figure 2C) that A431 cells express HER2 receptors and they are also rapidly activated by EGF treatment in a dose-dependent manner. Higher concentrations are necessary to maintain elevated phosphorylation levels over 24 hours. Sustained activation of EGFR and HER2 can affect a wide range of downstream signaling pathways producing varied outcomes on cellular processes.

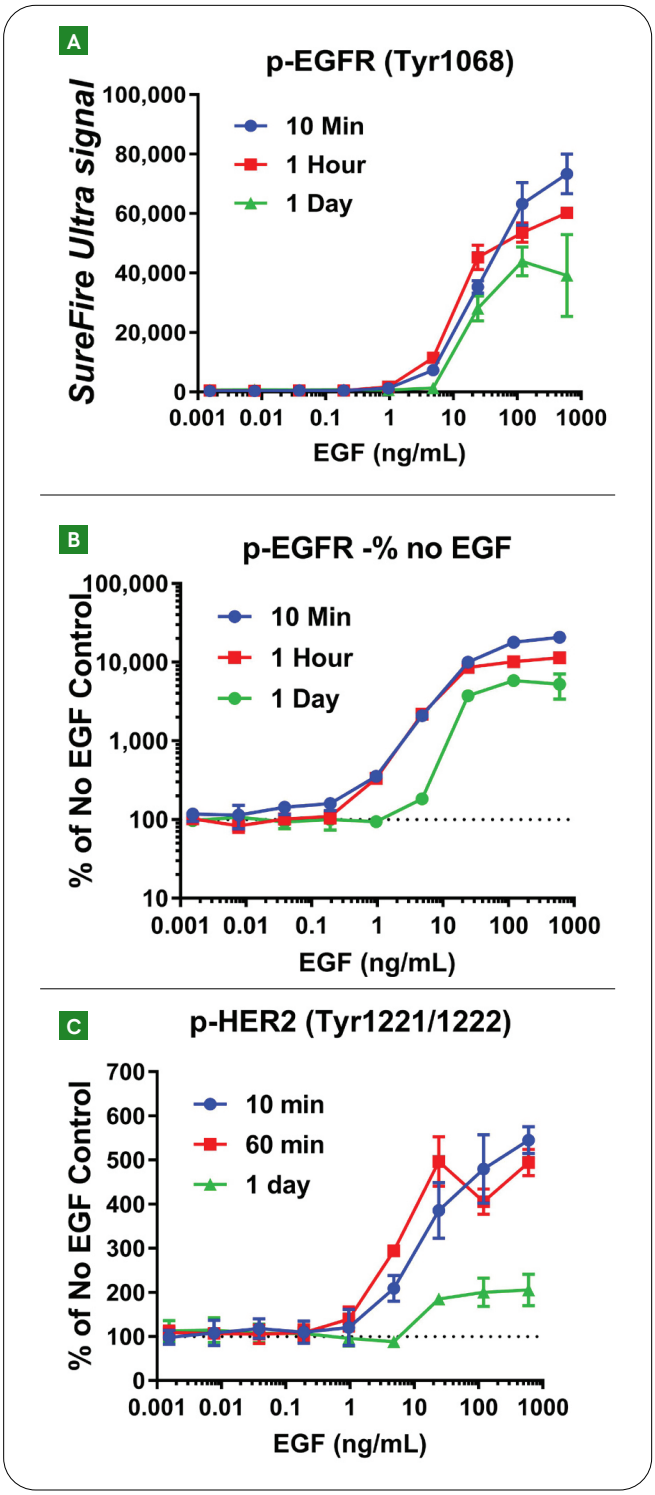

Figure 2. **AlphaLISA *SureFire Ultra* assays detect EGFR and HER2 phosphorylation potentiated by increasing concentrations of EGF over time.** A) Cells were treated with a broad range of EGF concentrations for 10 minutes, one hour, and one day and raw AlphaLISA signals detected indicating increased phosphorylation of EGFR at Tyr1068 site with increased EGF concentration. B) In order to compare timepoints, raw data were normalized as a percent of no EGF control wells and graphed on a log-log scale. C) Relative levels of phospho- HER2 were also detected from separate wells and indicate EGF treatment potentiates HER2. All data = average of 3 wells with SD as error bars.

Assessing EGF effects on downstream signaling pathways

Rapid activation of MEK/ERK and p38MAPK pathways

EGFR activation has been linked to the activation of numerous downstream signaling pathways, many which lead to changes in gene transcription.[6] One pathway long-associated with EGFR signaling is Ras-Raf-MEK-ERK,[7] an important pathway that interacts with over a hundred substrates to regulate a wide array of physiological responses, including growth, proliferation, differentiation, migration and apoptosis. To assess the effects of EGF on the activation of this pathway, cells were stimulated for multiple durations with a titration of EGF, lysed, and frozen. Plates were thawed and AlphaLISA *SureFire Ultra* assays for phospho-MEK1 (at Ser218/222) and p-ERK1/2 (Thr202/Tyr204) were run concurrently. The data in Figure 3A and 3B illustrate that the MEK and ERK pathways are rapidly activated by EGF with maximal activation of MEK1 occurring more rapidly than ERK1/2. MEK/ERK phosphorylation levels were potentiated over one hour with mid-range concentrations of EGF (around 1 ng/mL), whereas higher concentrations show decreased activation over one hour and all EGF-dependent effects diminished by the next day.

Another mitogen-activated protein kinase (MAPK) associated with EGFR signaling is p38 MAP kinase,[8] which has been shown to mediate EGF-dependent effects on STAT1 activation, growth inhibition, and apoptosis in A431 cells.[9] In our cultures, we see rapid p38 MAPK activation and maximal phosphorylation after 20 minutes with highest concentrations of EGF (Figure 2C), whereas heightened phosphorylation levels are not sustained overnight, much like the pattern observed with MEK/ERK.

Concentration and time-dependent effects on the PI3K/AKT pathway

PI3K/AKT is another primary pathway activated by EGF and influencing many different cellular processes, including cellular metabolism, growth, migration, and protein synthesis. EGFR phosphorylation stimulates AKT translocation and phosphorylation at two conserved residues, Thr308 and Ser473, and maximal activation is achieved by phosphorylation at both sites.[10] In order to observe a robust effect of EGF treatment on levels of p-AKT1/2/3, more cells were necessary. The number per well was doubled to 20,000 cells producing a significant signal to background, while maintaining a less-than confluent culture (data not shown). Testing different cell concentrations is an important early step in developing any cell-based assay,

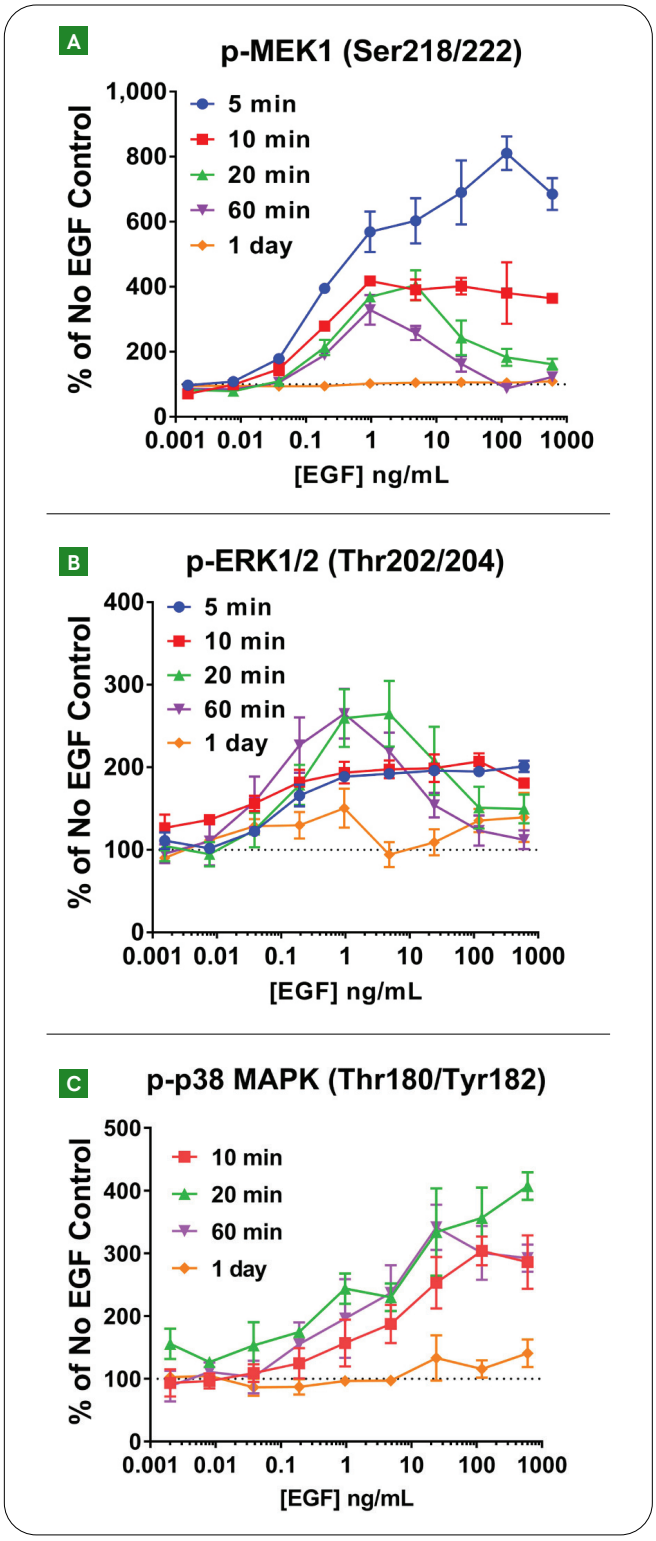

Figure 3. **Fast activation of the Ras-Raf-MEK-ERK pathway and p38 MAPK with EGF treatment.** Time-course analysis of EGF concentrations effects on levels of (A) p-MEK1 (Ser218/Ser222), (B) p-ERK1/2 (Thr202/Thr204), and (C) phosphorylation of p38 MAP kinase (Thr180/Tyr182). To determine effects relative to no treatment, data was converted to percent of no EGF control.

including AlphaLISA *SureFire Ultra* (for more guidance on cell-based assay development, see the AlphaLISA *SureFire Ultra* Assay Optimization Guide).[11] When examining treatment and time-dependent effects on AKT phosphorylation, there appears to be a bimodal response with different patterns at different treatment times (Figure 4A, 4B). A maximal effect of EGF at 1 ng/mL is observed at 20 to 60 minutes which disappears overnight. However, higher concentrations of EGF (25 ng/mL and greater) produced a sustained or heightened effect on p-AKT levels overnight. To determine whether the higher levels of AKT phosphorylation overnight were due to overall increases in AKT protein concentration, total levels of AKT1/2/3 were measured and results (Figure 4C) indicate EGF effects on levels of p-AKT are not due to changes in total AKT protein.

AKT mediates a wide range of physiological responses through activation or deactivation of several downstream kinases. One such kinase is GSK-3β which, in response to EGF, is phosphorylated at Ser9 and inactivated, allowing transcription and stabilization of Cyclin D1 which promotes cell cycle progression.[2] In our cultures, phospho-GSK-3β levels increased only after sustained EGF treatment at the higher concentrations that were shown to produce sustained levels of AKT phosphorylation overnight (Figure 4D).

STAT pathways and NF-κB activation

The Signal Transducer and Activator of Transcription (STAT) family of proteins are rapidly activated by a variety of growth factors and cytokines, affecting several different downstream processes through activation of gene transcription. STAT family members each play unique functions in signal transduction mediating cellular responses to different kinds of cytokines.[12] STAT family members, notably STAT3 and STAT5, are involved in cancer progression whereas STAT1 has been shown to suppress tumor growth in some models. All three have been shown to be rapidly activated by EGFR.[13] In our cultures, STAT1, STAT3 and STAT5 are all rapidly phosphorylated by EGF. Higher concentrations of EGF are needed to produce significant levels of p-STAT1 (Figure 5A) and p-STAT3 (Figure 5B), whereas phosphorylation of STAT5 (Figure 5C) is more sensitive and reaches maximal stimulation at lower concentrations with a greater sustained activation overnight than for STAT1 and STAT3.

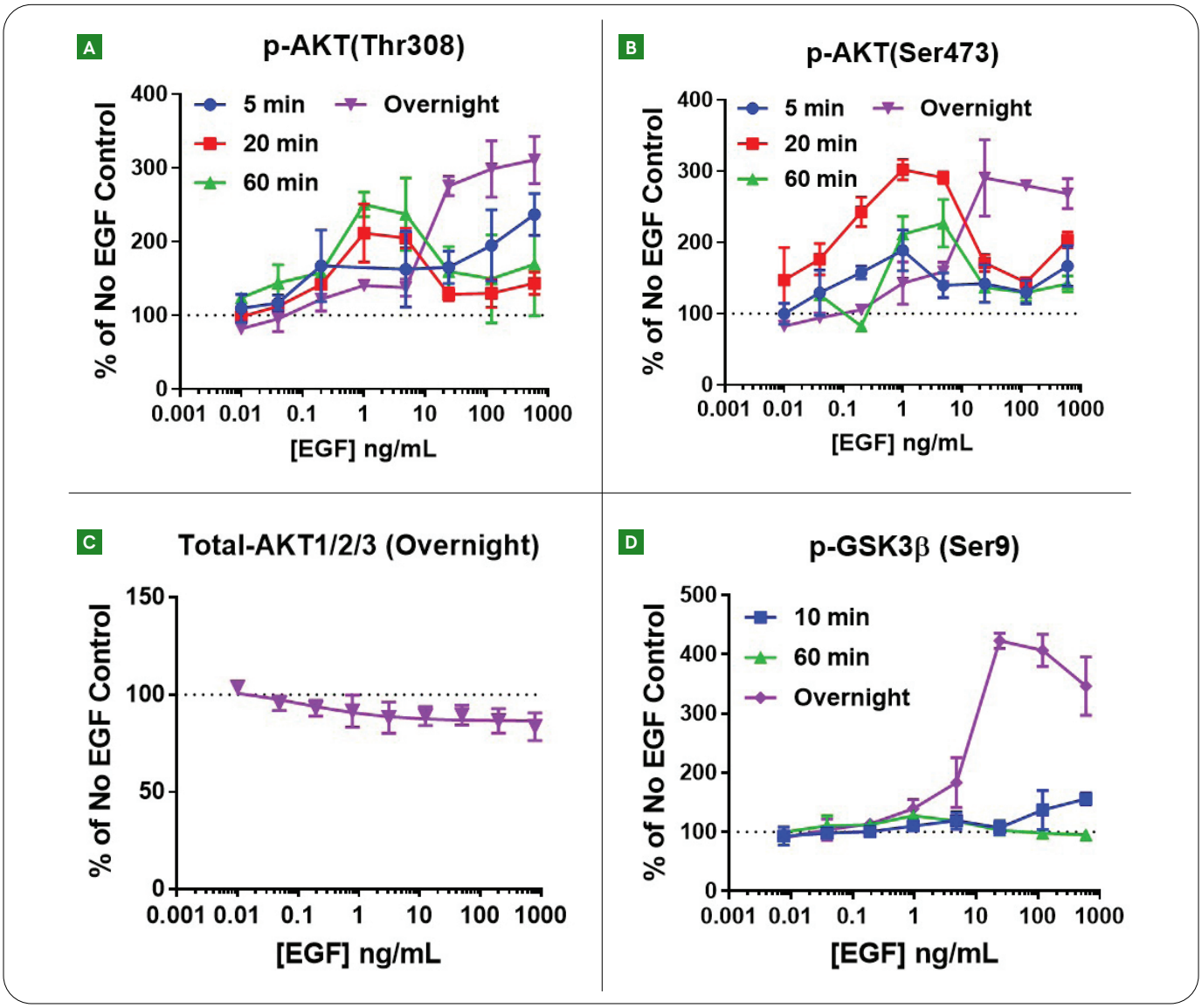

Figure 4. **Concentration and time-dependent stimulation of AKT phosphorylation and downstream effectors.** EGF optimally stimulates AKT phosphorylation at both (A) Thr308 and (B) Ser473 on different timescales depending on concentration but does not enhance (C) total AKT1/2/3 concentrations overnight. D) GSK3β phosphorylation increases after overnight stimulation with higher concentrations of EGF.

NF-κB (nuclear factor kappa-light-chain-enhancer of activated B cells) is a protein complex involved in DNA transcription, cytokine production and cell survival. It is present inactive in the cytosol and is rapidly activated by cytokines and other stimuli that causes it to then enter the nucleus and turn on expression of specific genes that regulate cell proliferation and survival. NF-κB turns on expression of its own repressor, forming an auto-feedback loop and resulting in oscillating levels of NF-κB activity. EGFR activation has been shown to rapidly activate NF-κB in A431 cells[14] and apoptosis to be accelerated if NF-κB is inactivated.[15] In our assay, we observe an increase in NF-κB phosphorylation in response to EGF stimulation, an effect that is not sustained overnight (Figure 5D), perhaps due to this auto-feedback loop.

As we've seen here, activation of the EGFR receptor results in the rapid and sometimes delayed or sustained stimulation of a number for different signaling pathways and transcription factors. These kinases and transcription factors have been shown to induce or inhibit a wide variety of cellular processes that regulate things like cell growth (size), morphometric changes (shape), chemotaxis (migration), cell cycle progression (proliferation and tumor progression), and cell death (apoptosis), as illustrated in the model in Figure 1A. For this reason, it is extremely important that treatment effects on these different processes are examined alongside pathway analyses in order to truly assess what's going on in the cell at these different time points and EGF concentrations.

EGF effects on cell health, growth and proliferation

ATP concentrations and cell numbers

There are many ways to assess treatment effects on cell health and proliferation. One way to examine both at once is by measuring relative levels of ATP, which acts as a surrogate marker for cell health and proliferation. We examined EGF effects on relative ATP concentrations per well using the ATPlite 1step luminescence assay after one hour and overnight treatment and data show both concentration and time-dependent effects (Figure 6A). EGF treatment for one hour actively depletes ATP at high concentrations (25 ng/mL and higher), whereas overnight treatment effects show ATP concentrations increasing relative to control wells in response to EGF concentrations from 10 pg/mL to 10 ng/mL. As ATP is needed to drive many cellular processes, the overall changes in ATP observed may be a result of maintaining phosphorylation of several intracellular pathways which, in turn, can affect cell growth and cell cycle progression (proliferation).

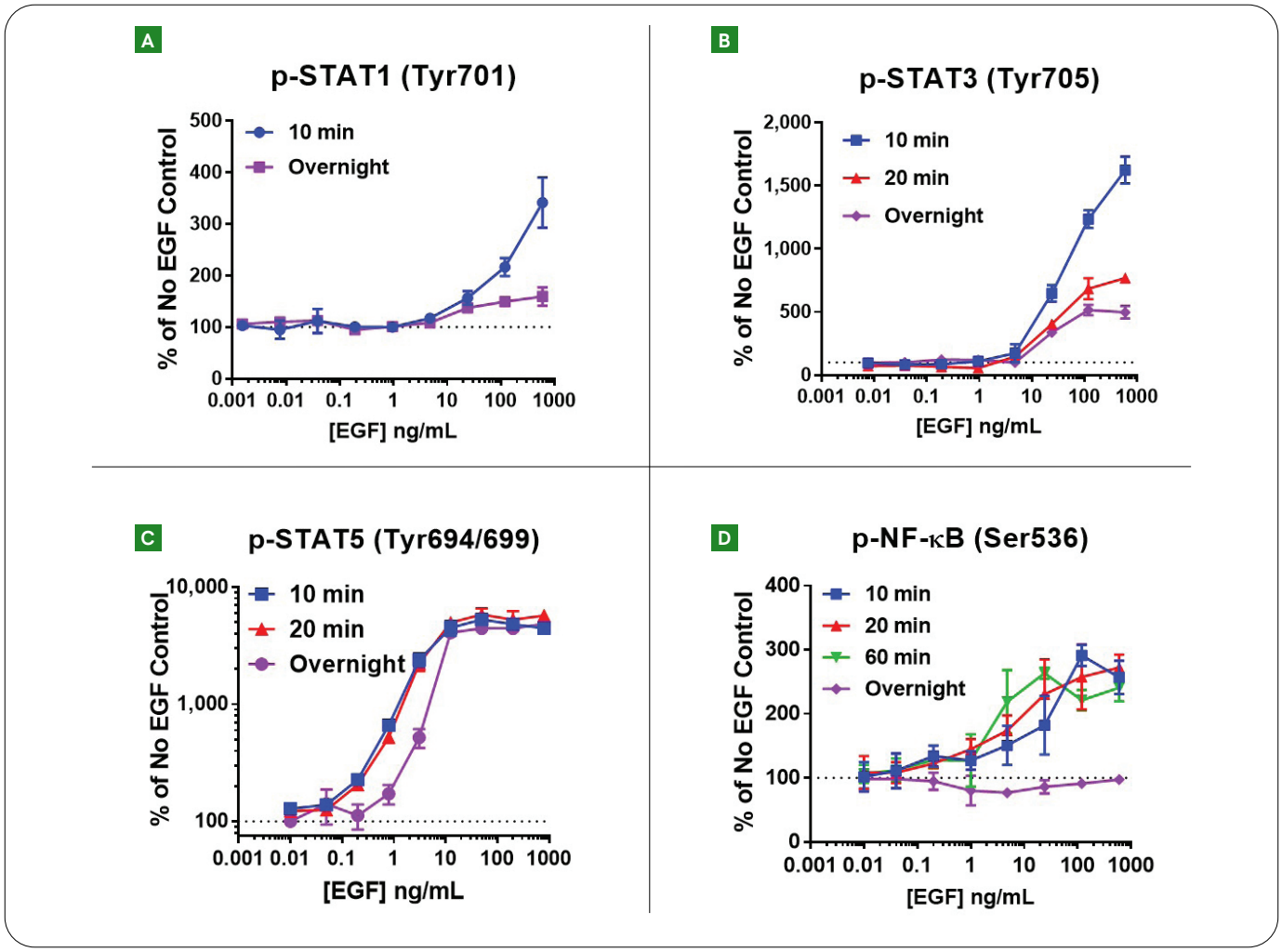

Figure 5. **Phosphorylation of STATs and NF-κB by EGF.** Effects of stimulation on phosphorylation of (A) STAT1, (B) STAT3, and (C) STAT5 were assessed at different time points showing rapid effects of EGF on levels of phosphoprotein which are at least partially sustained overnight. D) NF-κB phosphorylation is also rapidly phosphorylated by EGF, but the effect is not sustained overnight.

To assess whether changes in ATP were due to either changes in cell growth or cell number, cells were labeled with Hoechst 33342, imaged using the Operetta CLS system (Figure 6B), and the number of cell nuclei per well quantified with the Harmony software. The resulting normalized cell numbers (Figure 6C) indicate that the overnight effects of higher EGF on ATP is likely due to decreased cell numbers, which could be due to decreased proliferation or induced cell death. There were no clear effects on cell numbers at one hour of treatment. The increased ATP observed after overnight treatment (at middle concentrations) may be due to cell growth or the start of EGF-induced enhancement of cellular proliferation that has been reported at low EGF (pg/mL – ng/mL) concentrations.[16]

The presence of Ki-67 protein is an indicator of proliferative activity and is detected in the nucleus of cells during most stages of the cell cycle.[17] To assess this, cultures were fixed after overnight treatment and immunostained with a rabbit monoclonal antibody to Ki-67 conjugated to AlexaFluor 488 and the nuclear marker DAPI. Cells were imaged and the PhenoLOGIC™ machine learning feature was used to select the Ki-67+ cell population in the Harmony software (illustrated by green outlined cells in Figure 6D). The results of this experiment (Figure 6E) suggest a slight increase in proliferation overnight at lower concentrations of EGF that mirrors the results seen in ATP concentration and cell counts.

Confluency and cellular morphology

EGF treatment can promote changes in tumor cell motility and invasion and A431 cells have been reported to exhibit dramatic refractile morphologic changes and detachment from an extracellular matrix upon EGF treatment within as little as 30 minutes.[18] In order to measure these effects, cultures treated with varying concentrations of EGF for 1 hour or overnight were labeled with Hoechst (15 minutes before imaging), imaged using brightfield and UV fluorescence optics, and culture confluency (the percent of total well area covered by cells) was assessed. The resulting image analyses are shown in Figures 7A and 7C. Overnight treatment data are similar to that observed by ATP quantification and counting cell numbers (Figure 6). However, after only one hour of treatment, though there is no effect on cell number, there is a clear decrease in confluency in wells treated with 25 ng/mL EGF or more, an effect also seen in ATP concentrations. This rapid effect is striking and clearly illustrated in images (Figure 7B) taken before (left) and after 1 hour with 25 ng/mL EGF (right). Changes in confluency can be indicative of effects on cell cycle (proliferation), cell death (apoptosis), or changes in cellular growth (cell size). To assess whether EGF treatment affects cell size, cells were labeled with DAPI for cell counting and MitoTracker™ Deep Red to identify cell boundaries for measuring cell size (Figure 7D). This experiment indicates that the effects observed on culture confluency appear to be reflective of EGF-induced changes in individual cellular morphology and size.

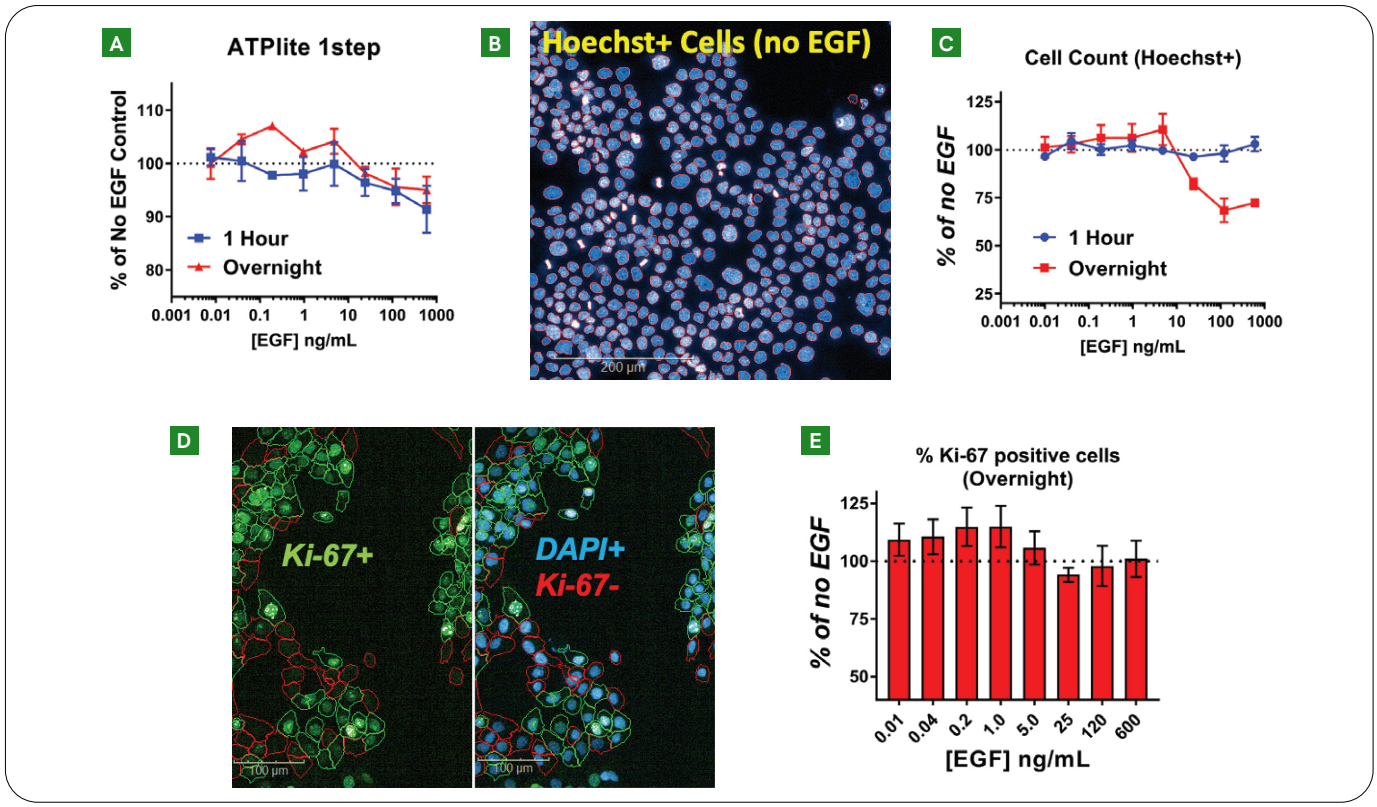

Figure 6. **EGF treatment eff ects on cellular ATP concentration and total cell numbers per well shown by imaging analysis.** A) Levels of cellular ATP were assessed at one hour and overnight using ATPlite 1step and data normalized to No EGF Control wells (dotted line). B) A431 cells treated with EGF were labeled with Hoechst (15 minutes), regions of each well were imaged on the Operett a CLS system with brightfield and UV fluorescence optics, nuclei identified (red outlines) and counted using Harmony soft ware. C) Cell numbers are signifi cantly lower with overnight treatment with higher concentrations of EGF compared to wells receiving no EGF. D) To determine the percent of dividing cells, cultures treated overnight were fixed and stained for Ki-67 and DAPI. Cells were imaged and Ki-67+ cells (green nuclei and outlines in left image) were distinguished from non-Ki-67+ cells (blue nuclei with red outlines seen in right image) using Harmony's PhenoLOGIC machine learning. E) Lower concentrations of EGF (overnight) result in a slightly higher percent of Ki-67+ cells (data is an average of two experiments, three wells/concentration in each).

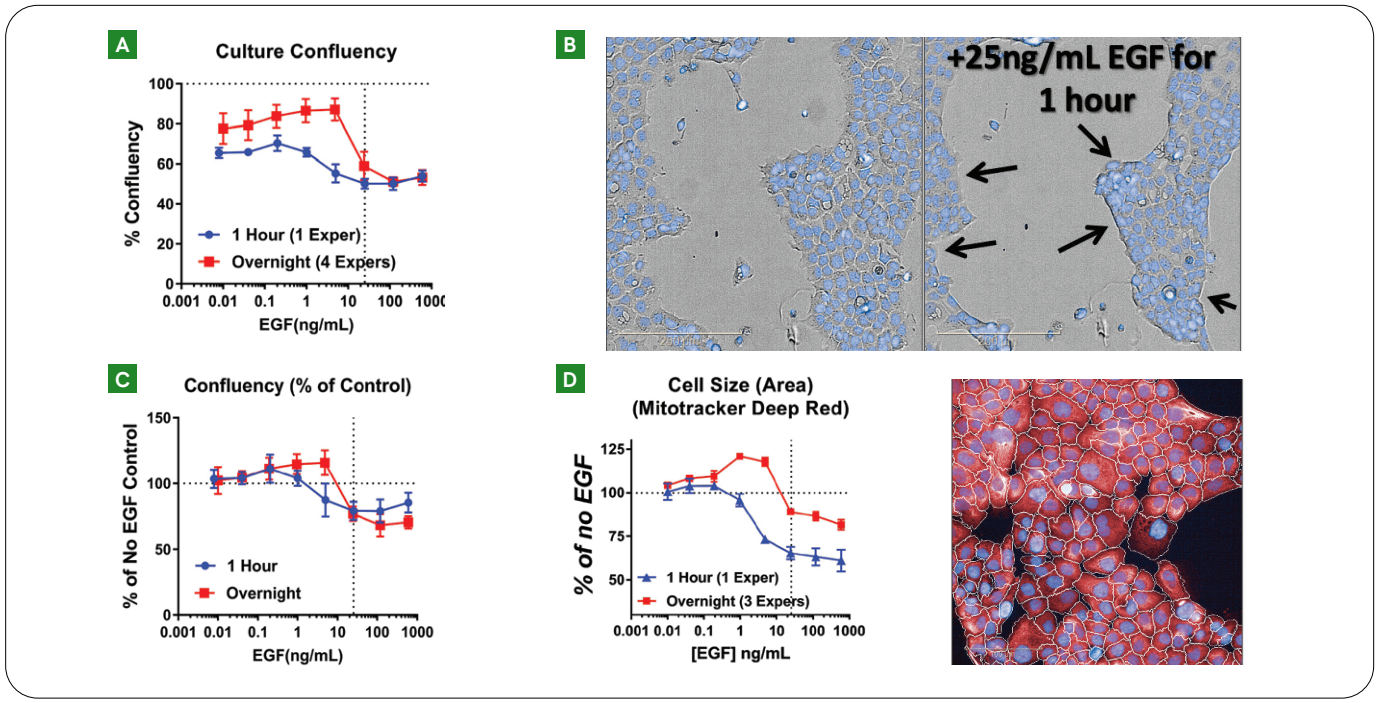

Figure 7. **EGF rapidly induces morphologic changes in cells that change with sustained treatment.** A) A431 cultures treated with EGF were labeled with Hoechst, imaged, and assessed for % Confluency. Th e horizontal line at 100% indicates that these cultures didn't become completely confluent and the vertical dotted line indicates 25 ng/mL EGF. B) A single well, labeled with Hoechst was imaged before (left image) and aft er treatment with 25 ng/mL EGF for one hour (right image). Arrows indicate cells changing shape and reductions in culture confluency. C) Data from (A) were normalized as a percent of control wells (100% line) to illustrate increases in confluency. D) To assess individual cell size, cultures were labeled with MitoTracker™ Deep Red, fixed and counterstained with DAPI (blue in image). A mask generated by finding the cytoplasmic outlines in the MitoTracker™ channel was used to measure cell size. Average cell size measures are indicated by the graph on the left (each experiment is an average of three wells).

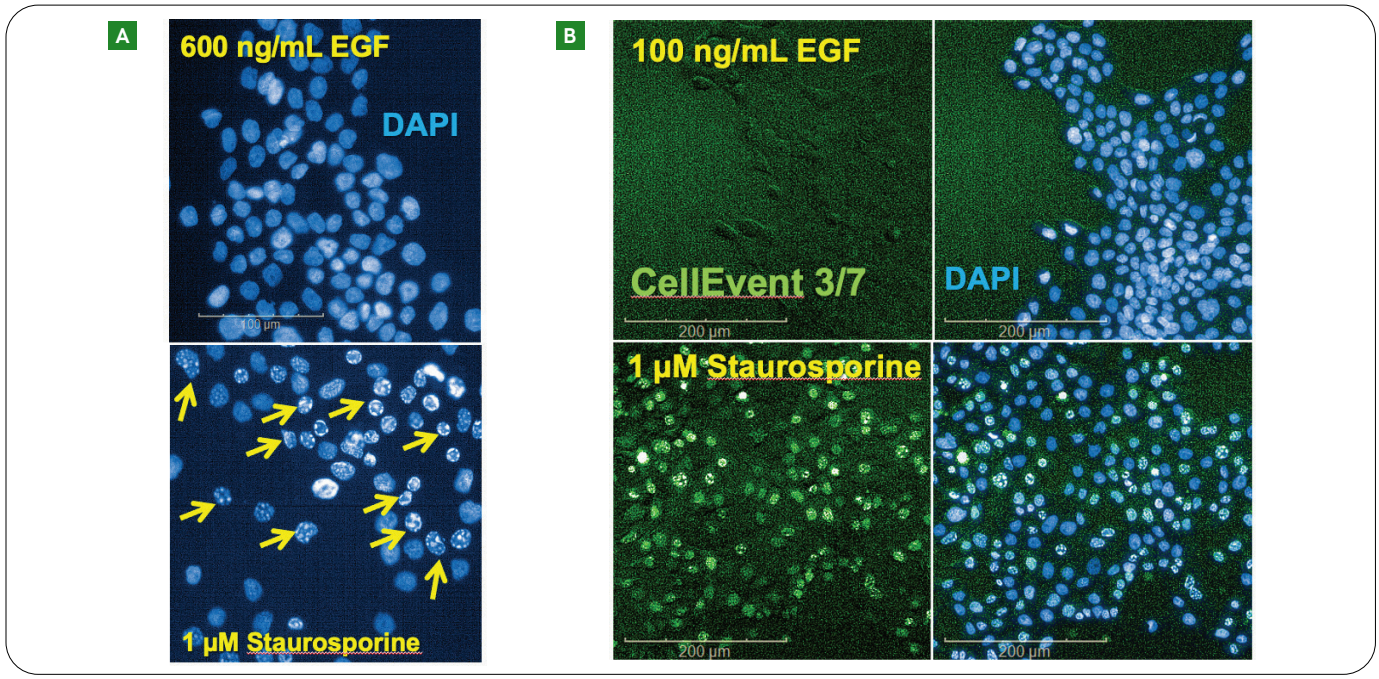

Figure 8. **Apoptosis not evident aft er overnight treatment with EGF (as opposed to with Staurosporine).** A) Wells were treated overnight with 600 ng/mL EGF (top) or 1 µM Staurosporine (bottom), fixed, and nuclei labeled with DAPI to show nuclear breakdown apparent in apoptotic cells which is evident in Staurosporine-treated cells. B) CellEvent™ Caspase-3/7 Green Detection Reagent was used to assess activity of Caspases 3 and 7 in cultures treated overnight with EGF (top) or Staurosporine (bottom). Green cells indicate Caspase activity in apoptotic cells and was only apparent in Staurosporine-treated wells.

Markers of Apoptosis

EGF treatment has been shown to promote changes in cell proliferation (cell cycle progression) and in cells that express high levels of EGFR, like A431 cells, promote apoptosis.[19] Apoptosis is a complex process of programmed cell death in which signaling events lead to characteristic changes in cellular morphology, including nuclear blebbing, cell shrinkage, nuclear fragmentation and chromatin condensation and DNA fragmentation. Nuclear blebbing and chromatin condensation can clearly be seen when examining cells labeled with nuclear dyes. Even after overnight treatment in highest concentrations of EGF, it is rare to find clear nuclear breakdown, whereas treatment with Staurosporine (1 µM), known to induce apoptosis, shows a clear effect as shown in Figure 8A.

Apoptosis usually involves the activation of caspases 3 and 7.[20] CellEvent™ Caspase-3/7 Green Detection Reagent is a fluorogenic cell-permeant substrate for activated caspases 3 and 7 consisting of a four amino acid peptide (DEVD) conjugated to a nucleic acid binding dye. After activation of caspase-3 or caspase-7 in apoptotic cells, the DEVD peptide is cleaved, enabling the dye to bind to DNA and produce a bright fluorogenic response (Exc/Em = 502/530 nm). When we examine our cultures after overnight treatment with EGF, even at highest concentrations, there is no clear caspase activity evident as opposed to that observed when wells are treated with Staurosporine (Figure 8B). These observations indicate that the overnight effects of high concentrations of EGF, observed on ATP concentrations, cell number and confluency, were due to changes in proliferation and not induction of traditional apoptotic mechanisms.

Conclusion

Treatment effects in cellular models not only drive changes in phosphorylation or expression levels of a target of interest but can also affect cellular health and proliferation, which can further influence the interpretation of downstream effects. In this application note, a model system using EGFR is presented to demonstrate how a complex cell-based assay can be developed and examined using a combination of cellular imaging and homogenous no-wash detection techniques.

Multiple downstream effects of EGFR stimulation, measured with AlphaLISA *SureFire Ultra*, are highlighted for several well-defined signaling pathways. AlphaLISA *SureFire Ultra* assays are an excellent approach for investigating several concentrations and time-dependent treatment effects on multiple signaling pathways. They are easy to use, provide high S/B, require small sample volumes, can be easily run concurrently, and are amenable to automation. Additional assays were run in parallel to determine cell health and proliferation effects including ATPlite and cellular imaging and analysis using the Operetta CLS high-content analysis system. ATP assessment and cellular imaging not only complement cell-based assays but provide more insight into affected cell processes both easily and rapidly with very little cost and preparation.

Complex pathway analysis can be rapidly assessed with high sensitivity upfront by using AlphaLISA *SureFire Ultra* while concurrently assessing higher level effects of treatment on cellular viability and growth using ATPlite and high content imaging and analysis.

References

1. Sigismund, S., et al. (2018). Emerging functions of the EGFR in cancer. *Molecular Oncology,* 12(1): 3-20.

2. Wee, P. and Wang, Z. (2017). Epidermal Growth Factor receptor cell proliferation and signaling pathways. *Cancers (Basel)*, 9(5): 52-96.

3. Idania, G., et al. (2017). Measurement of serum EGF levels, a methodological approach. *Journal of Molecular Biomarkers and Diagnosis,* 8(3).

4. Sette, G., et al. (2015). Tyr1068-phosphorylated epidermal growth factor receptor (EGFR) predicts cancer stem cell targeting by erlotinib in preclinical models of wild-type EGFR lung cancer. *Cell Death and Disease,* 6: e1850.

5. Meira, D.D., et al. (2009). Combination of cetuximab with chemoradiation, trastuzumab or MAPK inhibitors: mechanisms of sensitisation of cervical cancer cells. *British Journal of Cancer,* 101: 782-791.

6. Scaltriti, M., et al. (2006). The Epidermal Growth Factor Receptor Pathway: A Model for Targeted Therapy. *Clinical Cancer Research,* 2(18): 5268-72.

7. Silvy, M., et al. (1998). Differential dose-dependent effects of epidermal growth factor on gene expression in A431 cells. *Endocrinology,* 139(5): 2382-91.

8. Frey, M.R., et al. (2006). P38 MAP kinase regulates epidermal growth factor receptor downregulation and cellular migration. *The EMBO Journal,* 25: 5683-5692.

9. Kozyulina, P.Y., et al. (2013). p38 MAP kinase enhances EGF-induced apoptosis in A431 carcinoma cells promoting tyrosine phosphorylation of STAT1. *Biochemical and Biophysical Research Communications,* 430(1): 331-5.

10. Jacobsen, K., et al. (2017). Convergent Akt activation drives acquired EGFR inhibitor resistance in lung cancer. *Nature Communications,* 8: 410.

11. AlphaLISA *SureFire Ultra* Assay Optimization. 2019. Revvity Start-up Guide.

12. Voerhoven, Y., et al. (2020). The potential and controversy of targeting STAT family members in cancer. *Seminars in Cancer Biology,* 60: 41-56.

13. Olayioye, M.A., et al. (1999). ErbB Receptor-induced Activation of Stat Transcription Factors Is Mediated by Src Tyrosine Kinases. *The Journal of Biological Chemistry,* 274(24): 17209-18.

14. Sun, L. and Carpenter, G. (1998). Epidermal growth factor activation of NF-kB is mediated through IκBα degradation and intracellular free calcium. *Oncogene,* 16: 2095-2102.

15. Anto, R.J. (2003). Inhibition of NF-κB sensitizes A431 cells to epidermal growth factor-induced apoptosis, whereas its activation by ectopic expression of RelA confers resistance. *The Journal of Biological Chemistry,* 278(28): 25490-8.

16. Kawamoto, T., et al. (1983). Growth stimulation of A431 cells by epidermal growth factor: Identification of high-affinity receptors for epidermal growth factor by an anti-receptor monoclonal antibody. Proceedings of the National *Academy of Sciences,* 80(5): 1337-1341.

17. Sun, X. and Kaufman, P.D. (2018). Ki-67: more than a proliferation marker. *Chromosoma,* 127(2): 175-186.

18. Lu, Z., et al. (2001). Epidermal growth factor-induced tumor cell invasion and metastasis initiated by dephosphorylation and downregulation of focal adhesion kinase. *Molecular and Cellular Biology,* 21(12): 4016-31.

19. Kim, K., et al. (2015). Epidermal growth factor-induced cell death and radiosensitization in epidermal growth factor receptor-overexpressing cancer cell lines. *Anticancer Research,* 35: 245-254.

20. Walsh, J.G., et al. (2008). Executioner caspase-3 and caspase-7 are functionally distinct proteases. *Proceedings of the National Academy of Sciences,* 105(35): 12815-19.

Revvity, Inc.
940 Winter Street
Waltham, MA 02451 USA
www.revvity.com